DEVELOPMENT OF A SPHERICAL STEPPER WRIST MOTOR

Kok-Meng Lee*, George Vachtsevanos and ChiKong Kwan***

* School of Mechanical Engineering
** School of Electrical Engineering
GEORGIA INSTITUTE OF TECHNOLOGY
ATLANTA, GA 30332

ABSTRACT

This paper presents the design concept of a new spherical stepper robotic wrist motor capable of three degrees of freedom (DOF) motion in a single joint for applications where high speed manipulation of end-effector orientation is required continuously in all directions. Typical applications are plasma and laser cutting and micro-assembly. The spherical motor is developed based on the principle of variable reluctance stepper motor. This paper high-lights the fundamental differences between the operation principle of 3 DOF spherical motor and that of the conventional stepper motor. The authors seek to establish a theoretic basis for design, prototype development and performance prediction. In particular, an analysis of torque prediction is discussed along with the presentation of kinematic and dynamic relationship. A laboratory prototype hybrid digital/analog control circuitry has been developed to demonstrate proof of concept feasibility and to assist in achieving an optimum design.

1. INTRODUCTION

Recent developments in robotics, data driven manufacturing and high precision assembly have provided the motivation for the resurfacing of unusual designs of electromechanical transducers. A flurry of research activity is currently underway in direct drives involving DC, stepping, and brushless electro-mechanical actuators to improve performance by eliminating the problems inherent in the gear systems such as backlash, friction due to meshing, and mechanical compliance. These devices are normally employed to accomplish a single degree of motion manipulation at each joint. An alternative design based on the concept of a spherical stepper wrist motor presents some attractive possibilities by combining pitch, roll, and yaw motion in a single joint. In addition to the compact design, the spherical wrist stepper motor results in relatively simple joint kinematics and has no singularities in the middle of the workspace except at the boundaries.

A spherical induction motor was designed, built and successfully tested by Laithwaite el at. [1-3]. The concept of a spherical motor was later employed in the design of a rotodynamic pump [4] and gyroscope applications [5-6]. The spherical induction motor combining a three DOF in-parallel mechanism as an approach to achieve fine motion dexterous manipulation was proposed in [7]. Although the theoretical basis of a field control spherical induction motor was performed in [8], realization of a prototype remains to be demonstrated. The mechanical design of a spherical induction motor is complex. Laminations are required to prevent movement of unwanted eddy currents. Complicated three phase windings must be mounted in recessed grooves in addition to the rolling supports for the rotor in a static configuration. These and other considerations lead to an investigation of alternative spherical actuators.

In this paper, the design concept of a spherical wrist motor based on the principle of variable reluctance (VR) stepper motor is presented. The spherical stepper motor combines pitch, roll and yaw motions in a single joint, which has significant potentials in applications where the demand on workspace is low but high speed isotropic manipulation of end-effector orientation is required continuously in all directions. Typical applications are high speed plasma and laser cutting and micro-assembly.

2. DESIGN CONCEPTS

A conceptual schematic of a spherical stepper motor is shown in Fig. 1. The motor consists of a hemispheric stator which houses the stator coils and a spherical rotor which houses a pair of permanent magnets. The rotor is supported freely by means of gimbals.

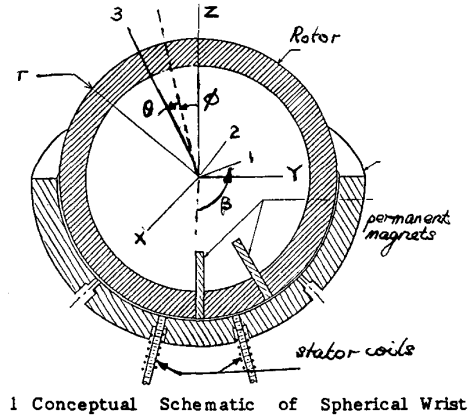

Figure 1 Conceptual Schematic of Spherical Wrist Motor

The spherical stepper motor operates on the principle of a VR motor. The stator coils can be energized individually using the control circuitry. As a pair of stator coils adjacent to the permanent magnets is energized so that a magnetic field and a corresponding flux is generated, the tangential components of the magnetic force attract the adjacent magnets and hence exert a resultant torque on the rotor. Appropriate sequencing of high current pulses which excite the stator coils results in the rotor producing a movement in any direction desired. The maximum torque generated and the motor resolution obtainable depend primarily on the geometry, the arrangement of the coils, the number of magnets as well as the m.m.f. through the coils.

The operation principle of the three DOF spherical stepper motor differs significantly from the single axis stepper motor. The primary difference is the required number of energized coils at any particular static orientation for mechanical stability and for three DOF motion control. As the conventional stepper motor is constrained physically to rotate about an axis, only one direction of actuating force is necessary to actuate or to lock the motion of the rotor in that direction. However, the spherical actuator has an infinite number of rotational axes and has three degrees of freedom. With only one energized coil, the permanent magnet considered to be a point on the rotor surface can be actuated in any direction along a tangent of the inner surface of the stator and thus provide two degrees of freedom motion control. The third DOF motion control, which is the spin motion about an axis through the center of the rotor and the point of attraction, may be provided through a second force of attraction between an additional active coil and a second permanent magnet generating an actuating torque perpendicular to the tangent surface. Hence, two forces which are not co-linear with the center of the rotor are necessary to provide rotor stability at a static position and 3 DOF motion at any instant.

The second difference refers to the fact that the maximum number of coils which can be evenly inscribed on a spherical surface is finite. The locations of the evenly spaced coils can be determined by building a polyhedron which is a three dimensional solid with polygons as faces (sides). For equal spacing, regular congruent polygons such as equilateral triangles, squares, or pentagons must be used. A point of a polyhedron makes up a convex polyhedral angle. Pythagoras and Plato [9] have shown that a complex polyhedran angle must be made up by at least three faces and must be less than 360° to form a closed polyhedron. Based on these principles, it can be shown that the maximum number of coils which can be evenly spaced on a sphere is 20 corresponding to the number of complex angles of a dodecahedron.

3. COIL ARRANGEMENT

More than 20 coils are typically required in order to achieve a high positional resolution. A scheme, therefore, was devised to space the coils on the lower hemisphere of the stator as evenly as possible. The position of every coil is represented by the following mathematical relation as illustrated in Fig. 2. The inner surface of the stator is described by the spherical surface ST, radius r, and the coil positions is represented by an array of points, CP. The spacing between points is set by the angular parameter θ which is in degree and is positive.

$$ST = \{ (x,y,z) : x^2 + y^2 + z^2 = r^2 ; \; Z \leq 0.0 \text{ and } x,y,z,r \in R \}$$

$$CP = \{ [(x,y,z), (i,j)] : \; (x,y,z) \in ST \text{ and } i,j \in I \}$$

$[(x,y,z), (i,j)] \in CP$ iff

$x = r \sin(i\theta)$

and

if $j = 0$ then

$y = 0$ and $z = -r \cos(i\theta)$

or if $j \neq 0$ there exist

$\{(a,b,c), [i,j-\text{sgn}(j)]\} \in CP$ s.t.

$(x,y,z) \cdot (a,b,c) = r^2 \cos\theta$

It has been shown that the least number of attractions required to provide locking of the rotor is two. For a given pair of magnets, the arrangement of the stator coils described above determines the primary resolution, which is defined by the spacing of the coils. Further improvement in resolution can be achieved by increasing the number of magnet pairs or modifying the radius of the rotor.

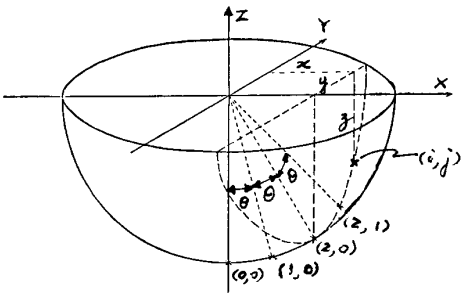

Figure 2 Schematic Illustrating Coil Arrangement

4. MATHEMATICAL MODEL

As shown in Fig. 1, an inertia coordinate frame, designated as XYZ frame is fixed at the center of the stator with its Z axis pointing towards the open-end of the stator hemisphere. Similarly, a body coordinate frame 123 is assigned to the center of the rotor, with its 3-axis pointing towards the center of the end-effector platform. The unit vectors along the (X,Y,Z) and (1,2,3) coordinates are designated as (I,J,K) and (i,j,k) respectively.

4.1 Kinematic relationship

The X-Y-Z Euler angles $q(\phi,\theta,\beta)$ is chosen to describe the orientation of the coordinate frame

123 with respect to the inertia frame, instead of the usual Z-Y-Z Euler angles because the Z-Y-Z Euler angles is indeterminate when the Z- axis and 3-axis coincide. The homogenous transformation [T] between the two coordinate systems is:

$$[i,j,k]^T = [T]\ [I,J,K]^T \qquad (1)$$

where

$$[T] = \begin{bmatrix} C_\theta C_\beta & S_\theta S_\phi C_\beta + S_\phi C_\phi & -S_\theta C_\phi C_\beta + S_\phi S_\beta \\ -C_\theta S_\beta & -S_\theta C_\phi C_\beta + C_\phi S_\phi & S_\phi C_\theta C_\psi + S_\phi C_\beta \\ S_\theta & -S_\phi C_\theta & C_\theta C_\phi \end{bmatrix}$$

where the subscripts of C and S are the angles of cosines and sines respectively. The Euler angle $q(\phi,\theta,\beta)$ is the general coordinate of the rotor. The angular velocity and acceleration of the rotor relative to the inertia frame can be described by the first and second derivatives of the $q(\phi,\theta,\beta)$, respectively. However, it will be more convenient to express the terms in vector form, with respect to the rotating frame, as far as dynamics concern. If the angular velocity of the body coordinate, ω, is:

$$\omega = \omega_1 i + \omega_2 j + \omega_3 k \qquad (2)$$

where

$$\omega_1 = \dot\phi\ C_\psi C_\beta + \dot\theta\ S_\beta$$

$$\omega_2 = -\dot\phi\ C_\theta S_\beta + \dot\theta\ C_\beta$$

$$\omega_3 = \dot\phi\ S_\theta + \dot\beta$$

The corresponding angular acceleration $d\omega/dt$ is :

$$\frac{d\omega}{dt} = \dot\omega_1\, i + \dot\omega_2 j + \dot\omega_3 k \qquad (3)$$

where

$$\dot\omega_1 = \ddot\phi\ C_\theta C_\beta + \ddot\theta\ S_\beta + \dot\theta\ \dot\beta\ C_\beta + \dot\phi\ \dot\theta\ S_\theta C_\beta - \dot\phi\ \dot\beta\ C_\theta S_\beta$$

$$\dot\omega_2 = -\ddot\phi\ C_\theta S_\beta + \ddot\theta\ C_\beta - \dot\theta\ \dot\beta\ S_\theta S_\beta + \dot\phi\ \dot\theta\ S_\theta S_\beta - \dot\theta\ \dot\beta\ C_\theta C_\beta$$

$$\dot\omega_3 = \ddot\beta + \ddot\phi\ S_\theta + \dot\phi\ \dot\theta\ C_\theta$$

When the forward dynamic problem is of interest, i.e. prediction of the rotor orientation $q(\phi,\theta,\beta)$ for a given external moment applied on the rotor, the conversion from the vector components to the Euler angle $q(\phi,\theta,\beta)$ is desire. The conversion equations have been derived as follow:

$$\left.\begin{aligned} \dot\phi &= \frac{1}{C_\theta}\ (\omega_1 C_\beta + \omega_2 S_\beta) \\ \dot\theta &= \omega_1 S_\beta - \omega_2 C_\beta \\ \dot\beta &= \omega_3 - \tan\theta\ (\omega_1 C_\beta - \omega_2 S_\beta) \end{aligned}\right\} \qquad (4)$$

4.2 Dynamic model

Unlike a single axis motor, the dynamic equations of the three DOF spherical motor are coupled and non-linear. The dynamics equations are derived from the principle of conservation of angular momentum. If the design of the rotor is such that the 1,2, and 3 coordinate axes are the principle axes, i.e $I_{12} = I_{23} = I_{13} = 0$, the equations will be reduced to:

$$\left.\begin{aligned} M_1 &= I_1 \dot\omega_1 + (I_3 - I_2)\ \omega_2\ \omega_3 \\ M_2 &= I_2 \dot\omega_2 + (I_1 - I_3)\ \omega_1\ \omega_3 \\ M_3 &= I_3 \dot\omega_3 + (I_2 - I_1)\ \omega_2\ \omega_1 \end{aligned}\right\} \qquad (5)$$

where $\mathbf{M} = [M_1\ M_2\ M_3]^T$ is the external moment applied on the rotor about its C.G. and can be expressed as:

$$\mathbf{M} = T(q, \dot q, \ddot q) + F(\dot q) + M_l(q)$$

where T is the actuating torque vector generated by the magnetic system F and M_l are the friction and load torque vector respectively. Rearrange equation (5) as a system of first order differential equations as follow:

$$\left.\begin{aligned} \dot\omega_1 &= \frac{1}{I_1}\ [(I_2 - I_3)\ \omega_2\ \omega_3 + M_1] \\ \dot\omega_2 &= \frac{1}{I_2}\ [(I_3 - I_1)\ \omega_1\ \omega_3 + M_2] \\ \dot\omega_3 &= \frac{1}{I_3}\ [(I_1 - I_2)\ \omega_2\ \omega_1 + M_3] \end{aligned}\right\} \qquad (6)$$

Whereas Equation (2), (3) and (5) determines the actuating torque required given the orientation trajectories, Equation (4) and (6) together form a state space representation of the forward dynamics. The state variables are the Euler angles $q(\phi,\theta,\beta)$ and the angular velocity, with respect to frame 123, ω and the input is the external moment M.

4.3 Torque Prediction

The torque generated by the magnetic system is derived from the principle of conservation of energy, which yields:

$$\dot E_m(t) = \dot E_e(t) - T(t) \bullet \omega(t) \qquad (7)$$

where

$\dot E_m$ = time rate of increase in magnetic energy stored,
$\dot E_e$ = electrical power input
= $i(t).\dot\lambda(t)$
i = current through the coil,
λ = flux linkage through the coil,
T = resultant torque acting on the rotor,
ω = angular velocity of the rotor.

Since the Magnetic Energy is a function of the configuration of the magnetic system, i.e. the coil current, relative position of the rotor, functions will be expressed in terms of the Euler angle $q(\phi,\theta,\beta)$.

The torque components in the directions of $dq(\phi,\theta,\beta)/dt$ is found first and, then, resolved in to the three orthagonal components in the 123 direction. It is derived that the dot product of the torque $T=[T_\phi, T_\theta, T_\beta]$ and the angular velocity ω is:

$$T \bullet \omega = (T_\phi + S_\theta T_\beta)\ \dot\phi + T_\theta\ \dot\theta + (T_\beta + S_\theta T_\phi)\ \dot\beta \qquad (8)$$

The time derivatives of the energy terms, E_m and E_e, are partial differentiated with respect to the Euler Angles, ϕ, θ, and β. With the constant

$$[T_\phi + T_\beta S_\theta + \frac{\partial E_m}{\partial \phi} - \Sigma\,(i\,\frac{\partial \lambda}{\partial \phi})]\,\dot{\phi}$$

$$+\ [T_\theta + \frac{\partial E_m}{\partial \theta} - \Sigma\,(i\,\frac{\partial \lambda}{\partial \theta})]\,\dot{\theta}$$

$$+\ [T_\beta + T_\phi S_\theta + \frac{\partial E_m}{\partial \beta} - \Sigma\,(i\,\frac{\partial \lambda}{\partial \beta})]\,\dot{\beta} = 0 \qquad (9)$$

Since this equality is true for any $[dq(\phi,\theta,\beta)/dt]$, it holds only when the coefficients of the velocity term are zero. Under this condition, three linear simultaneous equations in the torque components are obtained. The three torque components were solved for and are as follow:

$$T_\phi = \frac{1}{C_\theta^2}\,[\,S_\theta \frac{\partial E_m}{\partial \beta} - \frac{\partial E_m}{\partial \phi} + \Sigma i\,(\frac{\partial \lambda}{\partial \phi} - S_\theta \frac{\partial \lambda}{\partial \beta})] \qquad (10)$$

$$T_\theta = \Sigma\,(i\,\frac{\partial \lambda}{\partial \theta}) - \frac{\partial E_m}{\partial \theta} \qquad (11)$$

$$T_\phi = \frac{1}{C_\theta^2}\,[\,S_\theta \frac{\partial E_m}{\partial \phi} - \frac{\partial E_m}{\partial \beta} + \Sigma i\,(\frac{\partial \lambda}{\partial \beta} - S_\theta \frac{\partial \lambda}{\partial \phi})] \qquad (12)$$

After transformation, the torque can be expressed in terms of three orthogonal vector components in the direction of frame 123.

$$T_1 = T_\phi C_\theta C_\beta + T_\theta S_\beta \qquad (13)$$

$$T_2 = -\,T_\phi C_\theta S_\beta + T_\theta C_\beta \qquad (14)$$

$$T_3 = T_\phi S_\theta + T_\beta \qquad (15)$$

4.4 Stored Magnetic Energy

Without loss of generality, the rotor is assumed to have two permanent magnets as shown in Figure 3 in the following analysis. In practice, the closed magnetic path can be realized by filling the rotor to a certain depth with iron trimmings, connecting the metallic cores of the coils by means of laminations, and allowing for a small stator coil spacing to ensure an overlapping area between the core and the magnet.

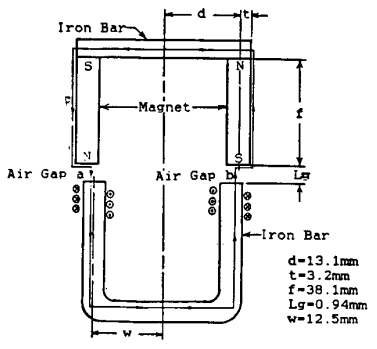

Figure 3 Schematic of the Magnetic System

As the permeability of the iron parts is generally large as compared to that of air gaps, the permeability of the iron parts in the system is assumed to be infinite. On the other hand, the flux linkage surrounding the magnets cannot be ignored as the permeability of the magnets is of the same order as that of the air. With these assumptions, the magnetic stored energy can be determined from an equivalent magnetic circuit which can be derived using Thevenin's Theorem. This yields :

$$E_m = \frac{1}{2}\,\Phi^2 R \qquad (16)$$

where Φ is the magnetic flux flow through the equivalent magnetic circuit with resultant reluctance, R. The reluctance is the reciprocal of the permeance which can be derived from the following equation :

$$P = \mu \int \frac{dA}{L} \qquad (17)$$

where μ is the permeability and dA is differential cross section area of the flux tude as a function of tude length, L. The arc-straight line method as suggested in reference [10] was used to model the air gap permeance based on the assumed flux patterns which were detailed in [11], where the integration was performed numerically. The magnet flux can be obtained by dividing the total m.m.f. of the magnetic circuit, which can be derived from Maxwell's equation along a closed-path for a specified magnet properties, by the reluctance.

5. STATIC TORQUE PREDICTION

It is generally expected that the magnetization curve of the magnets is non-linear. Thus, an experimental prediction of the reluctance forces using a pair of Neodymium permanent magnets (6mm X 6mm X 38mm) was performed on the system as shown in Figure 3. The magnetic flux density of the magnet, B_m, is determined experimentally to be 0.7 Wb/m^2. The experimental data are displayed in Fig. 4 . The maximum force of 7 N is obtainable with the current of 4 Amperes and 600 turns per coil on an iron bar of 1/4 inch diameter. Hence, with a spherical rotor of 125mm diameter, a maximum restoring torque of 0.44 Nm may be obtained. Also, a maximum force of 3 N is obtainable with no m.m.f. implying that repulsive force in addition to attractive force is necessary in the switching the magnet from one coil to the other.

Although the theoretical data which is computed using permeance-based model [10,11] does not match the measured force exactly, they are in qualitative agreement. In addition the model gives a reasonably good prediction of the location of the peak. The force-separation curves predicts the optimum spacing of 6mm between the stator coils, which results a maximum restoring torque to move the permanent magnet from one stator coil to another. Further increase of spacing between stator coils may result a non-recoverable condition due to the decay of restoring force with distance.

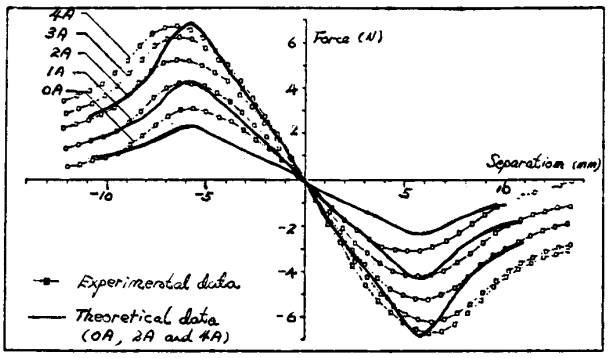

Figure 4 Predicted Reluctance Force

6. CONTROL CIRCUITRY

Two level of control scheme, coarse-fine motion strategy, is proposed for a pre-planned trajectory. The first level is the open-loop position control of the rotor teeth (permanent magnets) based on the switching circuitry for a pre-planned trajectory. In the second level, accuracy and stability are such important issues that the robust and fast convergent control algorithms should be applied to fine-motion control of the wrist motor. The following discusses the open-loop switching circuitry.

A hybrid digital/analog scheme has been developed in order to provide the appropriate sequencing and control functions of the spherical stepper motor. Although the design described in this section addresses a single permanent magnet - four stator coils case with corresponding movement in the spherically mapped x-y coordinate system, the extension to a multiple permanent magnet arrangement should follow similar guidelines. Emphasis was placed on designing circuitry that would provide maximum flexibility in allowing the implementation of a variety of activation schemes and the determination of the sensitivity to wrist parameter changes. Clearly the goal here is to realize a laboratory prototype that will assist in achieving an optimum design.

The digital control section consists of four parts: (a) a personal computer is used as a host for which current level microcontroller code is downloaded to a Motorola 68HC11 board serially via an RS232 port. The PC is basically used as a system input/output device. Its function is to receive operator commands and send their ASCII representation to the 68HC11. Finally, it receives and displays status messages consisting of echoing the stator movement to the screen. (b) A Motorola 68HC11 microcontroller in conjunction with a Motorola EVB board. The EVB board is used to facilitate communication with the PC and to provide additional ports as control lines. The 68HC11 receives commands from the operator terminal and performs the functions decoded. Current options are: move up, move down, move left, move right, and teach mode. Teach mode allows the user to program stator positions that are to be moved repeatedly. Stator coils are actuated only if the 68HC11 determines that the position is valid. The program converts the command into a stator address that is sent to the EPROM decode block via the PORT C bus lines. (c) An EPROM Decode Block which consists of a bank of six 2764 EPROMS loaded with stator firing positions to facilitate design flexibility. Each individual data line of this 2764's is used to control a specific stator coil. The current hardware configuration can control up to 48 stator coils. Changes in the number of coils to be controlled, the number of coils fired at a time, and the firing sequence can be handled by simply reprogramming the EPROM. (d) A Repulsion Flip-FLop Block - consisting of a 74L73 flip-flop with clear. Since a repulsion force is required whenever a stator coil is deactivated, there is one repulsion flip-flop circuitry allows control of three different logic states, attraction, repulsion and idle with only one control line and a global clear line for all flip-flops. This method thus allows control of N stator coils with N+1 control lines.

The analog section consists of three main parts: (a) An operational amplifier stage which connects directly to the outputs of the repulsion flip-flops and the EPROM. It generates the required positive and negative voltage levels for the stator attraction and repulsion modes, respectively. The square wave output is connected directly to the power transistor stage. (b) Bipolar Power Transistors provide current to the stator coils of up to two amperes when connected directly to the op amp output. Each stator coil employs two such transistors, one generating the positive current associated with attraction forces and the second generating the negative current associated with repulsion. The two transistors are configured in a push-pull format, with the stator coils connected as the load. (c) Stator coils which are energized by the power transistor outputs and controlled via the EPROM control lines. Each stator coil has currently three stable current states: +2 amps, -2 amps and zero amps.

The development software user a non-interactive version of the 68HC11 assembly code to keep complexity at a minimum. It allows for switching between different hardware configurations along with different firing sequences. Fig. 5 depicts the details of the microprocessor, EPROM and flip-flop connections. Fig. 6 shows the op amp and power transistor connections. Fig. 7 indicate the timing diagrams for the control and actuation signals.

7. CONCLUSIONS

The design concept of a new electromechanical spherical stepper wrist motor capable of 3 DOF motion in a single joint has been developed. Although the wrist motor is developed based on the principle of VR stepper motor, its operation principle significantly differs from that of the conventional single-axis VR stepper motor.

Along with the presentation of the kinematic and dynamic relationship, an analysis of torque prediction has been performed. Preliminary experimental torque prediction suggests that a maximum of 0.44 Nm restoring torque can be obtained with a pair of Neodymium permanent magnets (6mm X 6mm X 38mm) on a rotor of 125mm diameter although significant increase of restoring torque can be expected by increasing the permanent magnet pairs and/or the m.m.f. through the coils. However, the realization of an optimum design of a spherical stepper wrist motor is far from complete. Further work on prototype development, computer simulation and experimental verification of torque and resolution prediction are currently underway.

A laboratory prototype hybrid digital/analog control circuitry has been developed to assist in achieving an optimum design. The laboratory prototype performs well-showing proof of concept feasibility. Work underway is addressing the issues of multiple permanent magnet arrangement in order to achieve full 3 DOF motion and a variable current source for stator coil actuation and control purposes. Associated research tasks are exploring means for detecting the position of the rotor.

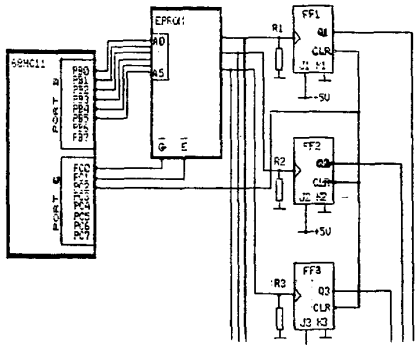

Figure 5 Microprocessor, EPROM and Flip-Flop Connection

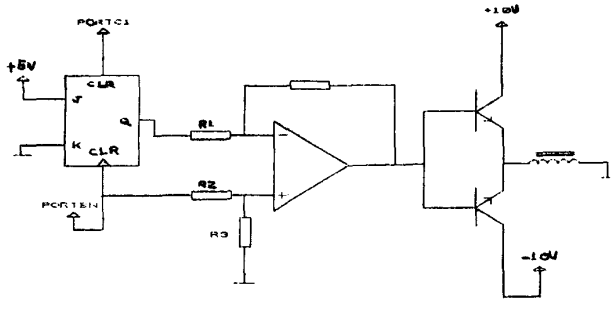

Figure 6 Op-Amp and Power Transistor Connection

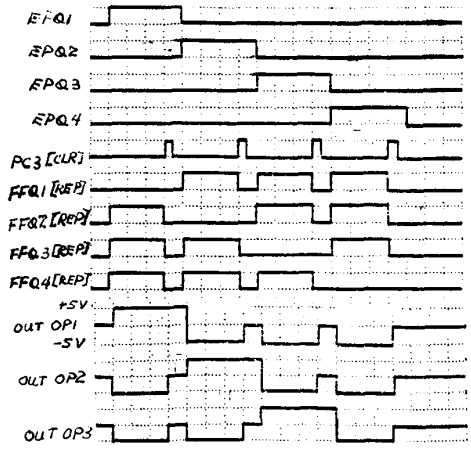

Figure 7 Timing digram for the signals produced by EPROM, Flip-Flop and Op-Amp outputs.

ACKNOWLEGDEMENT

This research is supported by the General Research Fund of the School of Mechanical Engineering at Georgia Tech.

REFERENCES :

1. William, F., Laithwaite, E., and Piggot, L., "Brushless Variable-Speed Induction Motors," Proc. IEEE, No. 2097U, pp.102-118, June 1956.
2. Williams, F., Laithwaite, E., and Eastham, G. F. "Development of Design of Spherical Induction Motors," Proc. IEEE, No. 3036U, pp. 471-484, December 1959.
3. Laithwaite, E., "Design of Spherical Motors," Electrical Times, vol. 9, pp. 921-925, June 1960.
4. Laing I. and Laing, N. Patent U.S. 4352646, Rotodynamic Pump with Spherical Motor, October 5, 1982.
5. Lebedev A. and Shinyev, P. "Moments Acting in a Spherical Rotor in a Magnetic Suspension," Priborostroegie, vol. 16, No.5 pp. 85-88, 1973.
6. Izv Vyssh Uchebn Zaved, "Electromagnetic processes in an Asynchronous Motor with a Spherical Hollow Rotor," Electromekh, N. 11, pp 1231-1239, Nov. 1976.
7. Vachtsevanos, G.J., and Davey K., and Lee, K. "Development of a Novel Intelligent Robotic Manipulator," Control Systems Magazine, June 1987.
8. Devay, K. and Vachtsevanos, G. "The analysis of Fields and Torques in a Spherical Induction motor," IEEE Trans. Mag., March 1987.
9. Smith, D. E., "Essentials of Plane and Solid Geometry," Wentworth-Smith Mathematical Series, 1923
10. Chai, H. D."Permeance Model and Reluctance Force Between Toothed Structures. Theory and and Applications of Step Motor edited by Kuo B.C.; West Publishing Co. 1973.
11. Kwan, C. "An Investigation of a Spherical Robot Wrist Actuator," MS Thesis (Mechanical Engineering) Georgia Institute of Technology 1987.